Journal of Systems Engineering and Electronics
Vol. 31, No. 6, December 2020, pp.1186 – 1192

# Detection and recognition of LPI radar signals using visibility graphs

WAN Tao*, JIANG Kaili, LIAO Jingyi, TANG Yanli, and TANG Bin

School of Information and Communication Engineering, University of Electronic Science and Technology of China, Chengdu 611731, China

**Abstract:** The detection and recognition of radar signals play a critical role in the maintenance of future electronic warfare (EW). So far, however, there are still problems with signal detection and recognition, especially in the low probability of intercept (LPI) radar. This paper explores the usefulness of such an algorithm in the scenario of LPI radar signal detection and recognition based on visibility graphs (VG). More network and feature information can be extracted in the VG two-dimensional space, this algorithm can solve the problem of signal recognition using the autocorrelation function. Wavelet denoising processing is introduced into the signal to be tested, and the denoised signal is converted to the VG domain. Then, the signal detection is performed by using the constant false alarm of the VG average degree. Next, weight the converted graph. Finally, perform feature extraction on the weighted image, and use the feature to complete the recognition. It is testified that the proposed algorithm offers significant improvements, such as robustness to noise, and the detection and recognition accuracy, over the recent researches.

**Keywords:** detection, recognition, visibility graph (VG), support vector machine (SVM), k-nearest neighbor (KNN).

**DOI:** 10.23919/JSEE.2020.000091

## 1. Introduction

Low probability of intercept (LPI) [1] radar signal detection and recognition technology is a research hotspot in recent years. Signal detection is the premise of electronic intelligent (ELINT), therefore, it is the basic content of radar signal reconnaissance theory research. And the signal modulation type has become an important direction of the electronic warfare (EW) research since 1980 [2], it is an important parameter for recognizing the working state of the radar. LPI radars have very low peak power, wide spectrum, high duty cycle, and low signal-to-noise ratio (SNR), making it difficult for EW receivers to detect and recognize them [3]. Therefore, the research on LPI radar signal detection and recognition is very important for future EW.

In recent years, many methods for recognizing LPI radar signals have been preprocessed by using time-frequency analysis. The purpose is to use new machine learning methods [4] in the time-frequency domain and recognize the generated signals [5−8], the recognition probability and the robustness to noise are getting good performance. However, the detection of LPI radar signals has rarely been proposed, and the basic idea is to recognize the detected signals. Moreover, the visibility graph (VG) research is also one of the hotspots in recent years. References [9, 10] proposed the VG and horizontal VG (HVG) method to convert time signals into complex networks. In [11], a method for rapidly converting time series into VG was proposed. In [12], the VG theory was introduced into the analysis of wall turbulence time series, which provides the strong support for accurate time series analysis of uneven turbulence. References [13,14] introduced a weighted complex network method based on VG, assigning a weight to each adjacent edge, and signal detection and recognition processing were performed on the obtained weighted complex network.

VG is periodic and it has a linear relationship with fractional Brownian motion and fractional Gaussian distribution [15,16]. For simple random sequences, HVG presents analytical solutions [10]. The reliability of converting white noise random sequences into VG was proved in [17]. The VG converted into the band-limited signal detection was introduced in [18], and the authors extracted the eigenvalues of the VG adjacency matrix for signal detection. In [19−22], VG theory was introduced into various types of signal recognition, the main idea is to convert the original random sequence into another domain that is easy to be processed by the matrix. The result is to promote the analysis and processing accuracy of the original sequence [22].

Manuscript received April 13, 2020.
*Corresponding author.
This work was supported by the National Defence Pre-research Foundation of China (30502010103).

This paper discusses the case of the LPI radar signals processing method based on the VG theory. Firstly, the signal received by the EW receiver is preprocessed. Preprocessing is a filtering algorithm based on the wavelet denoising principle (WDP). Then we obtain the power spectrum of the signal to be tested and compare it with the power spectrum of the additive white Gaussian noise (AWGN) signal. The real signal is detected. Secondly, the autocorrelation function is obtained for the detected signal, and the autocorrelation signal is converted into a VG network. Thirdly, we generate the weighted VG network and perform feature extraction. Finally, the support vector machine (SVM) and the $k$-nearest neighbor (KNN) [4] are used for signal modulation type recognition. The machine learning algorithm classifies the extracted features, including the modulation types of 14 LPI radar signals, which are monopulse (MP), linear frequency modulation (LFM), binary phase shift keying (BPSK), quadrature phase shift keying (QPSK), frequency shift keying (FSK), V-Shaped, LFM-BPSK, LFM-QPSK, Barker, Frank, and polyphase code (P1, P2, P3, P4).

The rest of this paper is organized as follows. Section 2 gives the expressions of the modulation types of each LPI radar signal and introduces the viewable method. The signal preprocessing algorithm and the VG weighting algorithm are overviewed in Section 3. Section 4 briefly describes the feature extraction. Section 5 is the validation of this paper including simulation experiment setup, results, and discussion.

## 2. Signal model

### 2.1 LPI radar signals

Assume that the radar pulse signal observation equation can be expressed as

$$\begin{aligned} y[k] &= x[k] + n[k] = \\ &[10pt]V \cdot \exp\{\mathrm{j}[2\pi f_c[k](kT_s) + \varphi[k]\} + n[k] \end{aligned} \tag{1}$$

where $y[k]$ represents the discrete-time signal intercepted by the EW receiver, $x[k]$ is the discrete-time complex radar signal, $n[k]$ is the complex AWGN, $V$ is the signal amplitude which is constant within a pulse width, $f_c[k]$ is the signal carrier frequency, $k$ is the sample index for each $T_s$ increase for the sampling frequency $f_s$, for a given pulse time interval $\tau_{pw}$, $0 \leqslant kT_s \leqslant \tau_{pw}$, and $\varphi[k]$ is the phase modulation function.

In practice, LPI radar signals are generally classified into three types: frequency modulation, phase modulation, and combined modulation. When the radar signal type is frequency modulation $f_c[k]$, the $\varphi[k]$ phase portion is constant; when the radar signal type is phase modulation $\varphi[k]$, the $f_c[k]$ frequency portion is constant [6], and the third one is frequency modulation and phase modulation combination. The 14 modulation types are shown in Table 1, including simple pulses, frequency modulation, phase modulation, and combined modulation.

**Table 1 Radar signal modulation type**

| Modulation type | $f_c[k]$/Hz | $\varphi[k]$/rad |
|---|---|---|
| MP | constant | constant |
| LFM | $f_0 + \frac{B}{\tau_{pw}}(kT_s)$ | constant |
| BPSK | constant | $(0, \pi)$ |
| QPSK | constant | $\left(0, \frac{\pi}{2}, \pi, \frac{3\pi}{2}\right)$ |
| FSK | $\{f_1, f_2, \cdots, f_{N_F}\}\}$ | constant |
| V-Shaped | $\begin{cases} f_0 + \frac{B}{\tau_{pw}}(kT_s),\ 0 \leqslant k < \frac{\tau_{pw}}{2} \\ f_0 + \frac{B}{2} - \frac{B}{\tau_{pw}}(kT_s),\ \frac{\tau_{pw}}{2} \leqslant k < \tau_{pw} \end{cases}$ | constant |
| LFM-BPSK | $f_0 + \frac{B}{\tau_{pw}}(kT_s)$ | $(0, \pi)$ |
| LFM-QPSK | $f_0 + \frac{B}{\tau_{pw}}(kT_s)$ | $\left(0, \frac{\pi}{2}, \pi, \frac{3\pi}{2}\right)$ |
| Barker | constant | (+1,+j,−1,+j,+1) |
| Frank | constant | $\frac{2\pi}{M}(i-1)(j-1)$ |
| P1 | constant | $-\frac{\pi}{M}[M-(2j-1)][(j-1)M+(i-1)]$ |
| P2 | constant | $-\frac{\pi}{2M}[2i-1-M][2j-1-M]$ |
| P3 | constant | $\frac{-\pi(i-1)^2}{N_c}$ |
| P4 | constant | $\frac{\pi(i-1)^2}{N_c} - \pi(i-1)$ |

### 2.2 VG and HVG

For VG, considering that the time series $S = \{t_1, t_2, \cdots, t_n\}$ is the sampling time of $n$ radar signals, without loss of generality, there are three arbitrary moments $a, b, c$, and $a < c < b$ is satisfied between them. If and only if one node can draw a straight line connecting $y_a$ and $y_b$, and a line does not intersect any intermediate reference "height" $y_c$, the two nodes $a$ and $b$ (assuming $a < b$ and without loss of generality) can be connected by a (non-directional) link line. According to the three criteria stated in [8], the following inequation is satisfied:

$$y_c < y_a + \frac{c-a}{b-a}(y_b - y_a), \ \ \forall c : a < c < b. \tag{2}$$

For HVG, similarly, if and only if a node can draw a horizontal line connecting $y_a$ and $y_b$, not intersecting any intermediate reference $y_c$, the two nodes $a$ and $b$ (assuming $a < b$ and without loss of generality) can pass one (non-directional) link line connection. According to the three criteria set out in [9], the following inequation is satisfied:

$$y_c < \inf(y_a, y_b), \ \ \forall c : a < c < b. \tag{3}$$

When the adjacent edges are connected, there are only two connections between M0 and M1 between any three nodes, which can be summarized as shown in Table 2 [15].

**Table 2 Sequential VG/HVG motifs sequence of three points**

| Motif | Criterion | |
|---|---|---|
| | M0  | M1 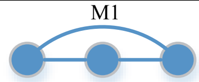 |
| VG | $\{\forall y_0, y_1 : y_2 \leqslant 2y_1 - y_0\}$ | $\{\forall y_0, y_1 : y_2 > 2y_1 - y_0\}$ |
| HVG | $\{\forall y_0, y_2 : y_1 > y_0\} \cup \{\forall y_0 : y_1 < y_0, y_2 < y_1\}$ | $\{\forall y_0 : y_1 < y_0, y_2 > y_1\}$ |

We can know that VG has periodicity from the definitions of VG and HVG, and at least one adjacent edge of the VG can be connected to the vertex. There are no isolated points, and boundary points will appear at the beginning and the end of the sequence [23–25]. The 14 kinds of LPI radar wave length determine the size, and VG and HVG adjacency matrix. If the time series has $n$ nodes and the adjacency matrix is $n \times n$, the adjacent matrix form is naturally different. For simple time series, HVG can obtain an analytical solution, assuming that the probability distribution of a random noise sequence is $p(n)(n \in [0,1])$, then $p(n) = \frac{1}{3}\left(\frac{2}{3}\right)^{n-2}$. For more general sequences, such as Markov sequences, $p(n)$ can also obtain analytical solutions [24]. Therefore, for LPI radar signals, under different sequence lengths, the VG adjacency matrix behaves differently, but they all have their own distribution methods. Within a certain range, the length of the size of VG or HVG matrix will make a little difference on recognition.

## 3. Preprocessing techniques

The algorithm illustrates the overall LPI radar signal detection and recognition technique proposed in this paper. The output is successful detection probability (SDP) and successful recognition probability (SRP).

**Algorithm** LPI radar signal detection and recognition algorithm

**Input** Signal to be tested through the AWGN channel

**Output** SDP, SRP

**Step 1** Give LPI radar parameters including sampling frequency $f_s$, code rate $f_b$, the number of symbols $N$, and $\{f_1, f_2, \cdots, f_{N_F}\}$ of FSK.

**Step 2** Wavelet denoising for the signal to be tested through the AWGN channel.

**Step 3** Convert the signal to be tested into VG or HVG.

**Step 4** Set the dynamic threshold for signal detection.

**Step 5** Perform autocorrelation for the detected real signal.

**Step 6** Weight the VG or HVG network.

**Step 7** Perform feature extraction on weighted complex networks.

**Step 8** Classify features by using SVM and KNN algorithms.

### 3.1 Signal preprocessing

LPI radar signals generally have low SNR characteristics, so reasonable noise reduction is one of the key technologies for signal detection and recognition. The essence of wavelet denoising is equivalent to signal filtering, and the interference noise is removed as much as possible under the premise of retaining LPI radar signals, which combines feature extraction and low-pass filtering. Set an appropriate threshold. When the high-frequency wavelet coefficients extracted after the time-domain signal processing are fewer than the threshold, the noise signal is considered to be removed; otherwise, the signal data greater than the threshold is retained as an effective LPI radar signal. Therefore, the suppression of LPI radar noise by wavelet transform is reasonable. In this paper, a signal detection method based on wavelet denoising is designed. Assume that the signal after through the AWGN channel can be expressed as

$$Y_i = S_i + \sigma Z_i,\ i = 1, \cdots, n \tag{4}$$

where $Y_i$ is the signal obtained after through the AWGN channel, $S_i$ is the original signal to be tested, $\sigma$ is the noise level, and $Z_i$ is the noise signal. The contaminated signal $Y_i$ is mostly the high-frequency signal. Using the principle that signals and noise have different characteristics under wavelet transform, a series of coefficients obtained after wavelet decomposition are processed, and the noise and signals are separated.

$$Y_i = A_1 + D_1 = A_2 + D_2 + D_1 = A_3 + D_3 + D_2 + D_1 \tag{5}$$

where $D_i$ is the high-frequency component of the decomposed signal, and $A_i$ is the low-frequency component of the decomposed signal. Usually, the low-frequency component is the most important, which can roughly reflect the characteristics of the signal, and the noise is generally distributed in the high-frequency component so that the signal and noise are separated. With the increase of the number of layers, the better noise suppression effect of the $A_i$ after wavelet decomposition is, the better the signal is obtained after wavelet inverse transformation. However, considering the amount of calculation and time cost, the number of layers is generally not too much. The essence of the algorithm is to reduce the wavelet coefficients generated by noise and retain the information of the original signal as much as possible.

### 3.2 Weighted complex network

The weighting algorithm [26] is to use the following equation for all adjacent edges of a vertex in a complex network, it can be expressed as

$$w_{ij} = \arctan \frac{n_j - n_i}{t_j - t_i},\ \ j > i \tag{6}$$

where $t_i$ and $t_j$ are the corresponding points of the time series, $w_{ij}$ is the weighted value of the joint node $n_i$ and the node $n_j$, and the weighted complex network algorithm is illustrated by taking three nodes as an example. Considering that the three nodes 1, 2, and 3 respectively correspond to values of 10, 15, and 25, then $w_{12} = \arctan \frac{15-10}{2-1} =$ 1.373 4, $w_{13} = \arctan \frac{25-10}{3-1} =$ 1.438 2, $w_{23} = \arctan \frac{25-15}{2-1} =$ 1.471 1.

## 4. Feature extraction

### 4.1 Average weighted degree

Consider the average weighting of a complex network as one of the best statistical attributes, because it is the most direct and most reflective factor of network complexity. It can be expressed as

$$aw = \sum_{j \in B(i)} w_{ij} \tag{7}$$

where $B(i)$ is the field of the node $i$. The average weighting of the network is the average of the total weight of all vertex connections in the network.

### 4.2 Average clustering coefficient

The average clustering coefficient reflects the clustering of the connection nodes, and its definition [26,27] can be written as

$$C_i = \frac{(M^3)_{ii}}{(M^2)_{ii}[(M^2)_{ii} - 1]},\ \overline{C} = \frac{1}{N}\sum_{i=1}^{N} C_i \tag{8}$$

where $C_i$ is the clustering coefficient of the node $i$, $M$ is the VG or HVG matrix, and $\overline{C}$ is the average clustering coefficient. This coefficient is directly processed by the network as a whole, therefore it is universal.

In addition, there are other features that can be used for LPI radar modulation type recognition, such as Newman coordination coefficient [28,29], normalized network structure entropy [30−32] and other features. However, in the application of this paper, adding more features has little effect on the improvement of the recognition effect, so we comprehensively consider the selection of the above two features.

## 5. Experimental results and discussion

### 5.1 Experimental setup

The experimental setup mainly includes LPI radar parameters setting. The value of sampling frequency $f_s$ is $5 \times 10^9$ Hz, the signal frequency $f_0$ is $1 \times 10^9$ Hz, the code rate $f_b$ is $2 \times 10^8$ Hz, the number of symbols $N$ is 6, the duration $\tau_{pw}$ is equal to $\frac{N}{f_b}$, the $\{f_1, f_2, \cdots, f_6\}$ of FSK is $\{10^9, 2\times10^9, 10^9, 2\times10^9, 10^9, 2\times10^9\}$. When the radar signal type is frequency modulation, the phase portion is constant, the value is 0; when the radar signal type is phase modulation, the frequency portion is constant, the value is $f_0$.

### 5.2 Detection

Convert the measured signal after wavelet denoising [33] into a VG adjacency matrix, and find its average degree. Similarly, we obtain the average degree of the noise signal. The false alarm probability $p_{fa}$ is set to 0.005, 500 Monte Carlo independent experiments are carried out, and the results are shown in Fig. 1.

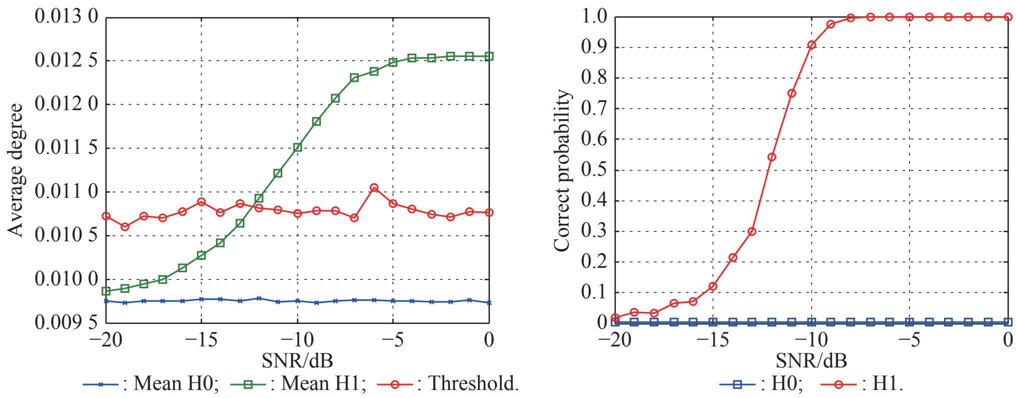


(a) Dynamic threshold setting under different SNRs (b) SDP

**Fig. 1 Signal detection simulation analysis**

The figure shows the average VG degree of signal passing through AWGN channel and after wavelet denoising processing. After setting the false alarm probabi lity, each threshold value in the SNR range of (−20,0) is obtained as shown in Fig. 1(a), and the detection probability of the signal is expected to be high. To solve the SDP, 500 times Monte Carlo experiments verify the detection probability as shown in Fig. 1(b).

In Fig. 1, when the SNR is −10 dB, the SDP is 90.9%, and as the SNR increases, the SDP also increases, especially when SNR>−8 dB, the SDP is basically 100%. Compared with [34], when the false alarm probability $p_{fa}$ is lower, the detection performance is still significantly improved. Therefore, we have enough reasons to believe that the detection algorithm is robust to noise. Also, the algorithm is currently only for LPI radar signals, and it is still applicable to the scenarios of acoustic signal processing and other signal processing.

### 5.3 Recognition

Modulation type recognition is performed on the detected signal. First, find the autocorrelation function of the signal and convert it to VG or HVG. The inverse Fourier transform of the signal is used to obtain the autocorrelation function, which is converted into VG or HVG. Then the VG complex network is weighted, and then features of the weighted network are extracted. Finally, the machine learning algorithm is used to recognize the features, including SVM and KNN [18]. The indicator for judging the classification performance mainly is the SRP. The performance of the different kernel functions of the SVM classifier is also different in the classification. Therefore, to evaluate the classification performance of these feature sets, we apply an additional SVM with radial basis function (RBF) kernel functions and an SVM with polynomial kernel functions. Similarly, consider KNN to experiment with different values of $K$ ($K$=3 and $K$=10) on the combined feature vector set. Their classification performance for 14 LPI radar signals is shown in Fig. 2.

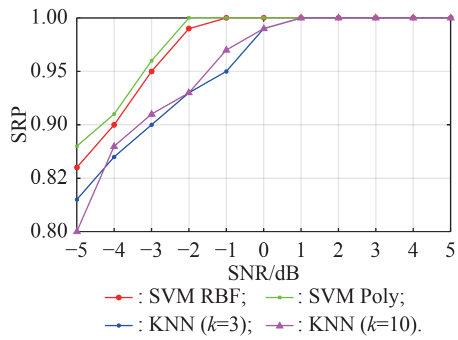


**Fig. 2 Classification performance of different classifiers**

Table 3 shows that the proposed algorithm is more accurate than the previous research. Among them, we only compare the overall experimental results with those using other existing methods and properly evaluate the SRP function.

The overall SRP of the algorithm proposed in this paper is 0.974, which is greatly improved compared with the previously proposed LPI radar waveform recognition technology. It is interesting to compare the following two situations: one is to improve the accuracy obtained by analyzing the time-frequency data processed manually, and the other is to improve the accuracy obtained by using the VG domain with complex network properties. Note that time-frequency analysis and deep learning require a lot of work and time, while the latter method requires very little engineering work and adds minimal computational cost. Introducing the VG idea into radar signal recognition is not only an attempt but also a new idea for the signal processing field. However, VG still has certain limitations. For example, because it is an undirected graph, if the signal amplitude and phase are the same, the amplitude linearly increases or decreases, and the converted VG is the same, such signals cannot be identified.

**Table 3 Comparison between the proposed algorithm and related studies**

| Source | Dataset | Method | Overall SRP |
|---|---|---|---|
| Reference [30] | 9 kinds of LPI radar waveforms | Time-frequency analysis+ multilayer perceptron (MLP) | 0.765 |
| Reference [8] | 9 kinds of LPI radar waveforms | Time-frequency analysis + Elman neural network (ENN) | 0.938 |
| Reference [31] | 12 kinds of LPI radar waveforms | Spectral correlation+ SVM | 0.887 |
| This paper | 14 kinds of LPI radar waveforms | VG+SVM+KNN | 0.974 |

## 6. Conclusions

This paper proposes an LPI radar detection and recognition algorithm based on the VG theory. The algorithm first performs signal noise reduction processing, and converts the noise-reduced signal into a VG complex network. Secondly it obtains the dynamic threshold by setting the false alarm probability of the VG average degree to complete signal detection. Then, the network extracts the features and uses machine learning algorithms to complete the LPI radar signal recognition. When the SNR is greater than −8 dB, the SDP is approximately 100%; and the SRP is nearly 100% when the SNR is greater than −2 dB. The experimental results also show that the average weighting and the average clustering coefficient are the most promising features for revealing LPI radar waveform hidden information when considering the weighted complex network theory. In future research, we will extend the VG theory to radar signal sorting and radar working pattern recognition applications.

## References


[1] PACE P E. Detecting and classifying low probability of intercept radar. Norwood: Artech House, 2009.

[2] SCHLEHER D C. Electronic warfare in the information age. Fitchburg: Artech House, 1999.

[3] WILEY R G. ELINT: the interception and analysis of radar signals. Fitchburg: Artech House, 2006.

[4] FU K. Applications of pattern recognition. Florida: CRC Press, 2019.

[5] HOANG L M, KIM M, KONG S H. Automatic recognition of general LPI radar waveform using SSD and supplementary classifier. IEEE Trans. on Signal Processing, 2019, 67(3): 3516–3530.

[6] KONG S H, KIM M, HOANG L M, et al. Automatic LPI radar waveform recognition using CNN. IEEE Access, 2018, 6: 4207–4219.

[7] KISHORE T R, RAO K D. Automatic intrapulse modulation classification of advanced LPI radar waveforms. IEEE Trans. on Aerospace and Electronic Systems, 2017, 53(2): 901–914.

[8] ZHANG M, LIU L, DIAO M. LPI radar waveform recognition based on time-frequency distribution. Sensors , 2016, 16(10): 1682.

[9] LACASA L, LUQUE B, BALLESTEROS F, et al. From time series to complex networks: the visibility graph. Proceedings of the National Academy of Sciences, 2008, 105(13): 4972–4975.

[10] LUQUE B, LACASA L, BALLESTEROS F, et al. Horizontal visibility graphs: exact results for random time series. Physical Review E, 2009, 80(4): 46–103.

[11] LAM X, MO H, CHEN S, et al. Fast transformation from time series to visibility graphs. Chaos: An Interdisciplinary Journal of Nonlinear Science, 2015, 25(8): 83–105.

[12] IACPBELLO G, SCARSOGLIO S, RIDOLFI L. Visibility graph analysis of wall turbulence time-series. Physics Letters A, 2018, 382(1): 1–11.

[13] SUPRIYA S, SIULY S, WANG H, et al. Weighted visibility graph with complex network features in the detection of epilepsy. IEEE Access, 2016, 4: 6554–6566.

[14] LACASA L. On the degree distribution of horizontal visibility graphs associated with Markov processes and dynamical systems: diagrammatic and variational approaches. Nonlinearity, 2014, 27(9): 20–63.

[15] SUPRIYA S, SIULY S, ZHANG Y. Automatic epilepsy detection from EEG introducing a new edge weight method in the complex network. Electronics Letters, 2019, 52(17): 1430–1432.

[16] GONCALVES B A, CARPI L, ROSSO O A, et al. Time series characterization via horizontal visibility graph and information theory. Physica A: Statistical Mechanics and its Applications, 2016, 464: 93–102.

[17] ZOU Y, DONNER R V, MARWAN N, et al. Complex network approaches to nonlinear time series analysis. Physics Reports, 2019, 787: 1–97.

[18] PAL S K, WANG P P. Genetic algorithms for pattern recognition. Florida: CRC Press, 1996.

[19] YAN K, WU H C, XIAO H, et al. Novel robust band-limited signal detection approach using graphs. IEEE Communica-

tions Letters, 2016, 21(1): 20–23.
[20] WAN T, FU X, JIANG K, et al. Radar antenna scan pattern intelligent recognition using visibility graph. IEEE Access, 2019, 7: 175628–175641.
[21] DU C, TANG B. Novel unconventional-active-jamming recognition method for wideband radars based on visibility graphs. Sensors, 2019, 19(10): 23–44.
[22] GAO Z K, CAI Q, YANG Y X, et al. Visibility graph from adaptive optimal kernel time-frequency representation for classification of epileptiform EEG. International Journal of Neural Systems, 2018, 27(4): 17S0005.
[23] DU C, ZHAO Y, WANG L, et al. Deceptive multiple false targets jamming recognition for linear frequency modulation radars. The Journal of Engineering, 2019, 2019(21): 7690–7694.
[24] LACASA L, JUST W. Visibility graphs and symbolic dynamics. Physica D: Nonlinear Phenomena, 2018, 374: 35–44.
[25] LACASA L, IACOVACCI J. Visibility graphs of random scalar fields and spatial data. Physical Review E, 2017, 96(1): 012318.
[26] NEWMAN M E. Scientific collaboration networks. I. network construction and fundamental results. Physical Review E, 2001, 64(1): 016131.
[27] IACOVACCI J, LACASA L. Visibility graphs for image processing. IEEE Trans. on Pattern Analysis and Machine Intelligence, 2019, 42(4): 974–987.
[28] NEWMAN M E, BARABASI A L E, WATTS D J. The structure and dynamics of networks. Princeton: Princeton University Press, 2006.
[29] SOFFER S N, VAZQUEZ A. Network clustering coefficient without degree-correlation biases. Physical Review E, 2005, 71(5): 57–101.
[30] LUNDEN J, KOIVUNEN V. Automatic radar waveform recognition. IEEE Journal of Selected Topics in Signal Processing, 2007, 1(1): 124–136.
[31] VANHOY G, SCHUCKER T, BOSE T. Classification of LPI radar signals using spectral correlation and support vector machines. Analog Integrated Circuits and Signal Processing, 2017, 91(2): 305–313.
[32] NEWMAN M E. Assortative mixing in networks. Physical Review Letters, 2002, 89(20): 208701.
[33] DONOHO D L. De-noising by soft-thresholding. IEEE trans. on Information Theory, 1995, 41(3): 613–627.
[34] YANG C, XIONG Z, GUO Y, et al. LPI radar signal detection based on the combination of FFT and segmented autocorrelation plus PAHT. Journal of Systems Engineering and Electronics, 2017, 28(5): 890–899.

## Biographies

**WAN Tao** was born in 1995. He received his B.S. degree from Harbin University of Commerce in 2017, Harbin, China. He is currently pursuing his Ph.D. degree with the University of Electronic Science and Technology of China. He is interested in electronic reconnaissance and is mainly engaged in electronic countermeasures, signal processing, and machine learning.
E-mail: taowan.uestc0939@foxmail.com

**JIANG Kaili** was born in 1991. She received her B.S. degree from the University of Electronic Science and Technology of China, Chengdu, China, in 2013. Currently, she is working toward her Ph.D. degree in the School of Information and Communication Engineering. Her research interests include wideband spectrum sensing, sparse/compressive sensing and radar signal processing.
E-mail: jiangkelly@foxmail.com

**LIAO Jingyi** was born in 1996. She received her B.S. degree from the University of Electronic Science and Technology of China, Chengdu, China, in 2018. She is currently pursuing her M.S. degree with the School of Information and Communication Engineering. Her research interest includes LPI radar signal detection and classification.
E-mail: LiaoJingyi@std.uestc.edu.cn

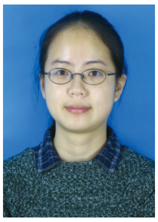

**TANG Yanli** was born in 1987. She obtained her bachelor's degree and master's degree in Chengdu University of Information Technology in 2010 and 2015, respectively. Currently she is pursuing her doctorate degree in the University of Electronic Science and Technology of China. Her major is information and communication engineering. Her research interests include radar countermeasure networks and radar signal reconnaissance.
E-mail: aaa123@yahoo.cn

**TANG Bin** was born in 1963. He is a professor of the University of Electronic Science and Technology of China. His research interests include complex/complex modulation LPI and new system radar reconnaissance and interference technology, adaptive radar reconnaissance and interference technology, networked radar countermeasure technology, broadband/ultra-wideband radar digital reconnaissance receiving and interference technology.
E-mail: bint@uestc.edu.cn